6-Sulfonylchromenes as Highly Potent K_{ATP}-Channel Openers

Ekkehart Salamon,[†] Raimund Mannhold,*[,‡] Horst Weber,[†] Horst Lemoine,[‡] and Walter Frank[§]

Institute of Pharmaceutical Chemistry, Heinrich-Heine-Universität, Universitätsstrasse 1, D-40225 Düsseldorf, Germany, Department of Lasermedicine, Molecular Drug Research Group, Heinrich-Heine-Universität, Universitätsstrasse 1, D-40225 Düsseldorf, Germany, and Institute of Inorganic and Structural Chemistry, Heinrich-Heine-Universität, Universitätsstrasse 1, D-40225 Düsseldorf, Germany

Received August 1, 2001

We synthesized K_{ATP}-channel openers (KCOs) composed of the 4-pyridonechromene moiety of bimakalim (**1**) and a variety of sulfonyl-containing 6-substituents **4**−**29**. Dilator potencies were measured in rat aorta and trachea. In both test systems the KCOs exhibit potency ranges of roughly 3 log units. The 6-*N*-phenyl-*N*-methylsulfonamido derivative **24** shows the highest potency. In rat aorta the potency spectrum ranges from a pEC_{50} value of 8.76 to 5.68; in rat trachea it ranges from 8.01 to 4.99. On average, the dilator activity is about 0.8 log units stronger in the aorta. Aortic relaxation by chromene **13** is markedly retarded, the clinical relevance of which (e.g., preventing tachycardia) remains to be clarified. Binding affinities were determined in myocardial membranes and aortic smooth muscle cells of the rat. The affinity spectrum in myocardial membranes ranges from a pK_D of 7.83 to 5.18; the highest affinity in aortic smooth muscle cells is measured for compound **28** ($pK_D = 8.55$), whereas the lowest affinity is measured for **4** ($pK_D = 4.51$). Significant selectivities discriminating between K_{ATP}-channels of different organs could not be detected. PLS analysis yielded no significant correlation between vasodilator activity in aorta and chemical descriptors (GRIND). Compounds **13**, **24**, and **28** represent the most potent KCOs of the 4-pyridonechromene type published so far. Their 6-substituents exhibit a phenyl ring with a congruent conformational orientation in relation to the sulfonylchromene. From SAR data and conformational analysis we postulate that these new 6-substituents extend the binding site for chromene KCOs. Correspondingly, we assume that the receptor area exhibits two separate interaction sites with the capacity to bind 6-substituents: (a) one site interacting with negatively polarized partial structures (e.g., CN, NO_2, SO_2) and (b) one spatially restricted site enabling favorable π-interactions.

Introduction

ATP-sensitive potassium channels (K_{ATP}-channels) are functionally and genetically members of the subfamily of inward rectifiers Kir.[1] Inward rectification is defined by a stronger inward conductance than outward conductance at a given membrane potential. K_{ATP}-channels differ from other inward rectifiers; in addition to the channel-forming α-subunit Kir, they include a regulatory β-subunit, the sulfonylurea receptor protein SUR.[2]

K_{ATP}-channels are ubiquituously distributed and exhibit a variety of physiological functions; the reduction of action potential duration[3] in cardiomyocytes,[4] the regulation of insulin secretion[5] in β-cells of the pancreas,[6] the control of vessel tone[7] in smooth muscle cells,[8] and transmitter release[9] in neurons[10] deserve mention here. Given their many physiological functions, K_{ATP}-channels represent promising drug targets. Both antagonists such as the antidiabetic sulfonylureas and agonists or openers of K_{ATP}-channels (KCOs) have been descibed.[11] Putative pharmacological applications of KCOs comprise hypertension, asthma, urinary incontinence, and cardiac ischemia to mention a few. The therapeutic usefulness of KCOs ultimately depends on their tissue selectivity. The existence and organ-specific distribution of isoforms of the K_{ATP}-channel forming subunits Kir (Kir 6.1[12] and Kir 6.2[13]) and SUR (SUR1,[14] SUR2A[15] and SUR2B[16]) might represent a rational basis for detecting tissue-selective KCOs. The identification of the KCO binding site on sulfonylurea receptors represents a further step into this direction.[17]

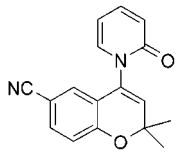

Bimakalim (1)

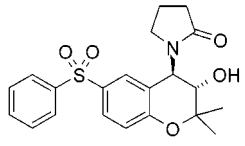

Rilmakalim (2)

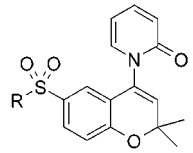

4 - 29

From the chemical point of view, currently available KCOs are extremely heterogeneous, comprising a number of different structural classes[18] of which the main three are the benzopyrans, the thioformamides, and the cyanoguanidines. The benzopyrans represent the most thoroughly investigated subgroup. Structure−activity studies[19] indicated that the 2-, 4-, and 6-positions of the benzopyran nucleus are highly susceptible to modulating the biological activity. Optimization of the 4-substituent led to the development of the bimakalim (**1**) series[20] characterized by a 4-pyridone moiety. Small electronegative substituents were long viewed as opti-

* To whom correspondence should be addressed. Phone: (0)211-8112759. Fax: (0)211-8111374. E-mail: Raimund.Mannhold@uni-duesseldorf.de.
[†] Institute of Pharmaceutical Chemistry.
[‡] Department of Lasermedicine, Molecular Drug Research Group.
[§] Institute of Inorganic and Structural Chemistry.

10.1021/jm010999g CCC: $22.00
Published on Web 02/01/2002

Scheme 1[a]

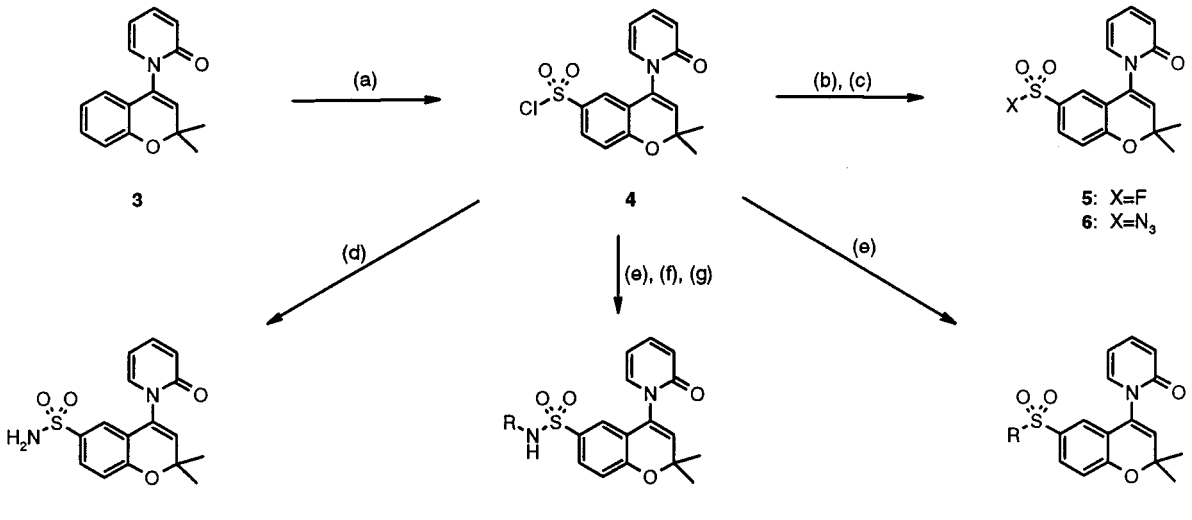

(e)	R
8	CH_3
9	C_2H_5
10	CH_2-CH_2-OH
11	$CH(CH_3)_2$
12	CH_2-C_6H_5

(f)	R
13	C_6H_5
14	C_6D_5
15	2-F-C_6H_4
16	2-Br-C_6H_4
17	4-Br-C_6H_4
18	4-OCH_3-C_6H_4

(g)	R
19	4-CN-C_6H_4
20	4-NO_2-C_6H_4

(e)	R
21	$N(CH_3)_2$
22	$N(C_2H_5)_2$
23	$N(CH_2$-$CH_2)_2O$

[a] Reagents and conditions: (a) chlorosulfonic acid, $CHCl_3$, −10 °C, 1 h; (b) KF, H_2O, 100 °C, 1 h; (c) NaN_3, EtOH + H_2O, 20 °C, 0.5 h; (d) NH_3 (gas), dioxane, 60 °C, 1 h; (e) corresponding amine (excess), dioxane, 20 °C, 0.5 h; (f) corresponding amine + triethylamine, dioxane, 20 °C, 0.5 h; (g) components melted at 85 °C (**19**) or 180 °C (**20**).

mal in the 6-position. The later development of rilmakalim (**2**) revealed that the introduction of a 6-phenylsulfonyl substituent significantly improved the vasodilator activity of benzopyran KCOs.[21] Additionally, within a series of new benzopyrans synthesized by our group,[22] 6-fluorosulfonyloxy substitution resulted in the compound with the highest vasodilator activity.

Thus, in the present study we synthesized structures (**4**−**29**) composed of the 4-pyridonechromene moiety of bimakalim (**1**) as a skeleton and of a wide variety of sulfonyl-containing substituents in the 6-position. A great many of the new structures represent sulfonamides (**7**−**24**, **29**), the rationale behind this being the pronounced chemical variability that can be achieved by substitution of two hydrogens. We investigated the biological activity of the compounds in four different test models. Structure−activity relationships were investigated via chemometric analyses.

Chemistry

Synthesis of sulfonylchromenes was accomplished according to the following procedures. Pyridone-substituted chromene **3** served as the starting material and was prepared as described previously.[22] Chlorosulfonylation in chloroform at low temperature gave high yields of the key intermediate **4**, which could be converted to the fluoride **5** or the azide **6** with an excess of the corresponding alkali salts in water or aqueous ethanol, respectively. The sulfonamide **7** was prepared by passing ammonia through a solution of **4** in hot 1,4-dioxane. *N*-Mono- and *N*-dialkylsulfonamides (**8**−**12**, **29**, and **21**−**23**) were synthesized by reaction of **4** with an excess of the corresponding amines in 1,4-dioxane at room temperature. Yields of aromatic sulfonamides **13**−**18** could be improved by addition of triethylamine. Both 4-aminobenzonitrile and 4-nitroaniline did not react with **4** under these conditions but gave the corresponding sulfonamides **19** and **20** when fused without a solvent at elevated temperatures (Scheme 1).

Scheme 2[a]

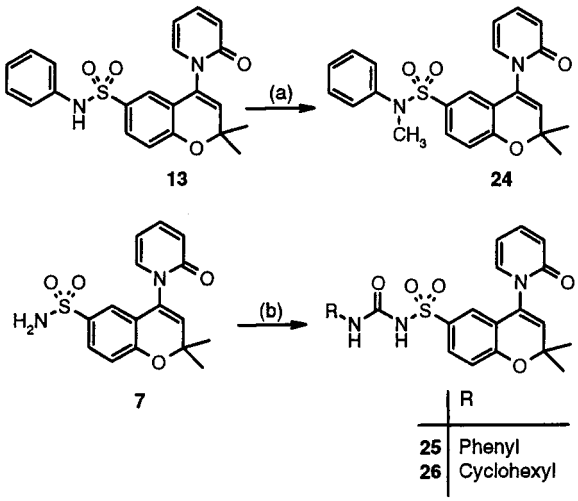

R	
25	Phenyl
26	Cyclohexyl

[a] Reagents and conditions: (a) CH_3I, NaOH, EtOH, 50 °C, 1 h; (b) R−NCO, NaOH, acetone, 20 °C, 1 h.

Methods for preparation of the remaining compounds are summarized in Schemes 2 and 3. Base-catalyzed methylation of anilide **13** gave better yields of **24** than direct sulfonylation of *N*-methylaniline with **4**. The synthesis of sulfonylureas **25** and **26** was achieved by addition of the corresponding isocyanates to the sulfonamide **7** under alkaline conditions. Yields were only

Scheme 3[a]

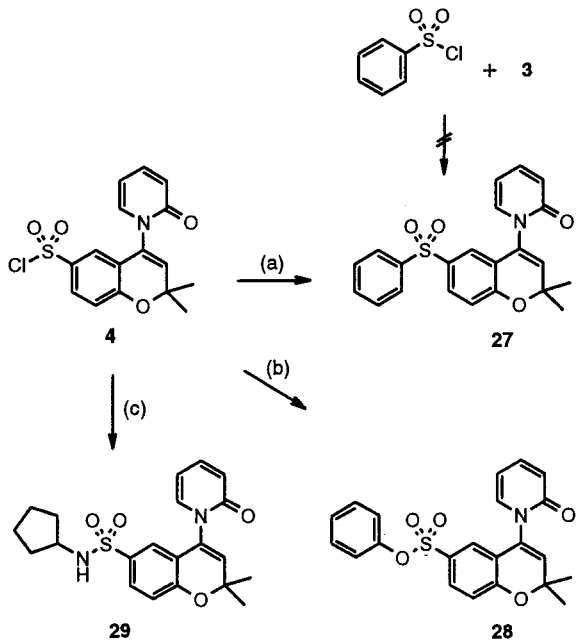

[a] Reagents and conditions: (a) benzene, $AlCl_3$, 20 °C, 1 h; (b) phenol, CH_2Cl_2, NaOH, benzyltrimethylammonium bromide, 40 °C, 6 h; (c) cyclopentylamine, dioxane, 20 °C, 0.5 h.

low, and purification of products by silica gel chromatography was necessary.

Attempts to synthesize the sulfone **27** from the Friedel−Crafts reaction of **3** with benzenesulfonyl chloride failed because only transformation of the chromene to an indene ring system was observed. However, sulfonylation of benzene with **4** was successful and gave the sulfone **27** in moderate yield. The ester **28** was prepared from **4** and phenol in dichloromethane/aqueous alkali using benzyltrimethylammonium bromide as a phase-transfer catalyst.

Stability of the compounds was tested in aqueous Krebs buffer solution as used in the biological experiments. Stock solutions (10^{-2} M) in DMSO (1 mL) were diluted with 20 mL of buffer and were stirred for 6 h at 32.5 °C. After addition of 50 mL of water, the solutions were extracted with ethyl acetate. TLC analysis of the organic and aqueous phases showed no sign of hydrolytic or other degradation products because only starting material could be detected. Even addition of dilute ammonium hydroxide (10%) to the Krebs buffer solutions of **4**−**6** at room temperature did not result in conversion to the sulfonamide **7**.

Results and Discussion

Because of the widespread therapeutic applicability of KCOs, including hypertension, asthma, and cardiac ischemia, we investigated the database molecules (structures are given in Table 1) in the following biological test systems: the binding affinities were determined in cardiac membranes for 27 compounds and in aortic smooth muscle cells of the rat for 24 compounds; the dilator properties were measured in rat aorta and trachea for 21 compounds. Details of the pharmacological assays are given in section B of the Experimental Section. The entire biological data are summarized in Tables 1 and 2.

Table 1. Binding Affinities of 6-Sulfonyl Varied Chromenes in Rat-Heart Myocytes and Aortic Smooth Muscle Cells[a]

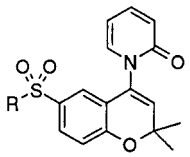

	R	heart pK_D[b] ± ASD	SMC pK_D[c] ± ASD	Δ[d] ± ASD
1	bimakalim	7.25 ± 0.03	7.98 ± 0.04	0.73 ± 0.05
2	rilmakalim	7.57 ± 0.03	8.15 ± 0.04	0.58 ± 0.05
5	F	7.83 ± 0.06	8.01 ± 0.07	0.18 ± 0.09
6	N_3	7.83 ± 0.12	not tested	
7	NH_2	6.50 ± 0.08	6.94 ± 0.04	0.44 ± 0.09
8	NH−CH_3	7.18 ± 0.05	7.26 ± 0.13	0.08 ± 0.14
9	NH−CH_2−CH_3	6.70 ± 0.06	7.00 ± 0.02	0.30 ± 0.06
10	NH−CH_2−CH_2−OH	6.16 ± 0.06	6.34 ± 0.05	0.18 ± 0.08
11	NH−$CH(CH_3)_2$	5.18 ± 0.05	5.08 ± 0.14	−0.10 ± 0.15
12	NH−CH_2−Ph	5.28 ± 0.08	6.00 ± 0.06	0.72 ± 0.10
13	NH−Ph	7.83 ± 0.04	8.05 ± 0.04	0.22 ± 0.06
14	NH−[D_5]-Ph	7.73 ± 0.05	8.13 ± 0.06	0.40 ± 0.08
15	NH−*o*−F−Ph	7.63 ± 0.12	7.96 ± 0.10	0.33 ± 0.16
16	NH−*o*-Br−Ph	6.86 ± 0.05	7.64 ± 0.04	0.78 ± 0.06
17	NH−*p*-Br−Ph	5.77 ± 0.05	6.65 ± 0.04	0.88 ± 0.06
18	NH−*p*-OCH_3−Ph	6.27 ± 0.07	6.61 ± 0.08	0.34 ± 0.11
19	NH−*p*-CN−Ph	5.50 ± 0.07	6.12 ± 0.06	0.62 ± 0.09
20	NH-p-NO_2−Ph	5.35 ± 0.08	5.80 ± 0.07	0.45 ± 0.11
21	N−$(CH_3)_2$	6.91 ± 0.09	7.20 ± 0.07	0.29 ± 0.11
22	N−$(CH_2$−$CH_3)_2$	6.45 ± 0.08	6.94 ± 0.11	0.49 ± 0.14
23	N−$(CH_2$−$CH_2)_2$−O	6.44 ± 0.08	6.73 ± 0.04	0.29 ± 0.09
24	N−(CH_3)-Ph	7.69 ± 0.05	7.87 ± 0.12	0.18 ± 0.13
25	NH−CO−NH−Ph	5.55 ± 0.06	not tested	
26	NH−CO−NH−C_6H_{11}	5.25 ± 0.05	not tested	
27	Ph	6.86 ± 0.07	7.19 ± 0.06	0.33 ± 0.09
28	O−Ph	7.78 ± 0.06	8.55 ± 0.06	0.77 ± 0.08
29	NH−cyclopentyl	5.85 ± 0.06	6.27 ± 0.04	0.42 ± 0.07
	mean ΔpK_D[d]			0.41 ± 0.05

[a] Binding affinities were determined as equilibrium dissociation constants (pK_D) in competition binding experiments, performed in quadruplicate. Affinity data for bimakalim and rilmakalim are from eight and three independent experiments in heart membranes and from five and four independent experiments in aorta. [b] Affinities in purified membranes of rat heart. [c] Affinities in cultured smooth muscle cells (SMC) of rat aorta. [d] ΔpK_D = differences between cardiac and aortic myocytes.

Some major conclusions from inspecting the biological data are illustrated in Figures 1−3. Disappointing results were obtained with **27** representing the pure hybrid of bimakalim (**1**) and rilmakalim (**2**); compound **27** binds less potently than bimakalim and rilmakalim both in cardiac membranes (Figure 1a) and in aortic smooth muscle cells (Figure 1b); this contrasts sharply with KCOs of the chromanol type, where rilmakalim (6-phenylsulfonyl) is profoundly more potent than lemakalim (6-cyano).

Very promising data, however, were obtained within the series of sulfonamides (**7**−**24**, **29**). The most potent member of this series is the phenyl derivative **13**. A drastic diminution in binding affinity is observed when replacing phenyl by alkyl substituents such as methyl (**8**), ethyl (**9**), and isopropyl (**11**), as shown in Figure 2a, or benzyl (**12**). The difference in potency is about 2.5 log units when comparing **13** and **12** (Table 1). With one exception (**15**), substitution of phenyl in compound **13** is followed by a profound reduction in affinity, as demonstrated by compounds **16**−**20** and shown for some examples in Figure 2b. In addition, this figure shows that high binding affinity is retained when replacing −NH− in **13** by −O− in **28**.

Table 2. Potencies for Relaxation of Aortic Rings and Tracheal Strips by 6-Sulfonyl Varied Chromenes[a]

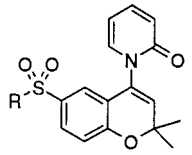

		aorta		trachea		
	R	pEC_{50}[b] ± SEM[c]	E_{max}[d] ± SEM,[c] %	pEC_{50}[b] ± SEM[c]	E_{max}[d] ± SEM,[c] %	ΔpEC_{50}[e] ± SEM[c]
1	bimakalim	7.79 ± 0.07	92.3 ± 1.2	6.80 ± 0.07	84.2 ± 3.1	0.99 ± 0.10
2	rilmakalim	8.62 ± 0.05[f]	81.2 ± 1.7[f]	7.57 ± 0.03[g]	78.5 ± 1.8[g]	1.05 ± 0.06
5	F	8.32 ± 0.08	84.4 ± 2.3	7.03 ± 0.03	90.5 ± 3.8	1.30 ± 0.09
6	N_3	7.79 ± 0.10	88.3 ± 3.1	6.69 ± 0.07	77.2 ± 5.2	1.10 ± 0.12
7	NH_2	7.16 ± 0.05	77.5 ± 2.3	6.65 ± 0.09	92.1 ± 1.4	0.51 ± 0.10
8	NH−CH_3	7.75 ± 0.04	85.8 ± 3.2	6.86 ± 0.06	83.0 ± 3.4	0.89 ± 0.07
9	NH−CH_2−CH_3	7.25 ± 0.06	72.4 ± 3.3	6.37 ± 0.02	87.0 ± 1.7	0.88 ± 0.06
10	NH−CH_2−CH_2−OH	6.96 ± 0.03	95.5 ± 3.7	6.00 ± 0.03	87.9 ± 2.7	0.96 ± 0.04
11	NH−$CH(CH_3)_2$	6.17 ± 0.06	76.9 ± 7.8	5.71 ± 0.10	94.8 ± 2.1	0.46 ± 0.12
12	NH−CH_2−Ph	6.28 ± 0.08	71.1 ± 2.2	5.88 ± 0.08	77.5 ± 2.5	0.40 ± 0.11
13	NH−Ph	8.51 ± 0.04	63.6 ± 4.4	7.85 ± 0.04	84.5 ± 2.0	0.66 ± 0.06
14	NH−[D_5]-Ph	8.70 ± 0.08	82.5 ± 3.3	7.88 ± 0.06	88.0 ± 2.0	0.82 ± 0.10
18	NH−*p*-OCH_3−Ph	6.93 ± 0.02	77.9 ± 5.8	6.31 ± 0.13	84.2 ± 7.0	0.62 ± 0.13
19	NH−*p*-CN−Ph	6.58 ± 0.05	84.0 ± 1.9	5.86 ± 0.03	90.8 ± 3.3	0.72 ± 0.06
20	NH−*p*-NO_2−Ph	5.68 ± 0.00	82.2 ± 1.5	4.99 ± 0.14	75.6 ± 2.2	0.69 ± 0.14
21	N−$(CH_3)_2$	7.79 ± 0.05	78.3 ± 2.6	7.02 ± 0.07	74.1 ± 3.1	0.77 ± 0.09
23	N−(CH_2−CH_2)$_2$−O	7.07 ± 0.05	75.5 ± 4.5	6.22 ± 0.08	85.1 ± 3.9	0.85 ± 0.09
24	N−(CH_3)−Ph	8.76 ± 0.06	64.2 ± 5.6	8.01 ± 0.02	86.5 ± 4.7	0.75 ± 0.06
25	NH−CO−NH−Ph	5.85 ± 0.05	90.8 ± 2.3	5.00 ± 0.09	99.5 ± 5.8	0.85 ± 0.10
27	Ph	7.76 ± 0.03	79.3 ± 2.1	6.74 ± 0.09	88.1 ± 5.4	1.02 ± 0.09
28	O−Ph	8.60 ± 0.06	67.9 ± 2.1	7.88 ± 0.01	86.7 ± 2.5	0.72 ± 0.06
	mean ΔpEC_{50}					0.81 ± 0.05

[a] Aortic rings were precontracted with 25 mM K^+. Tracheal strips were percontracted with 0.6 μM carbachol. [b] Dilator activity expressed as log of reciprocal half-maximal potency. [c] Standard error of the mean. [d] Maximum level of relaxation by the compound as percentage of basal tension. [e] Difference between the pEC_{50} values in rat aorta and trachea as an indicator of selectivity. [f] Jaspert and Lemoine, unpublished results. [g] Extrapolated from EC_{50} values (−log, M) for rilmakalim after precontraction with 0.2 μM carbachol (EC_{50} = 7.84 ± 0.02) and 2 μM carbachol (EC_{50} = 7.30 ± 0.03). For details, see text.

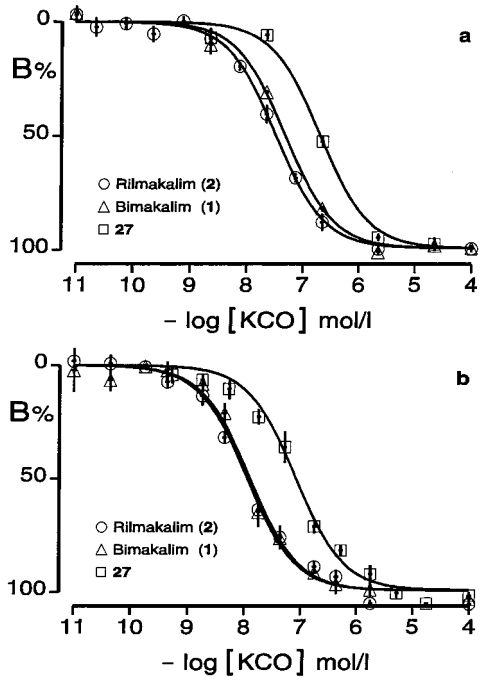

Figure 1. Binding affinities of rilmakalim **2**, bimakalim **1**, and their hybrid **27** in myocardial membranes (a) and cultivated smooth muscle cells (b). Assay conditions are given in section B of Experimental Section. Nonnormalized data (n = 4) were subjected to nonlinear regression according to eq 1, resulting in estimates of the dissociation constants (pK_D). Corresponding values are given in Table 1.

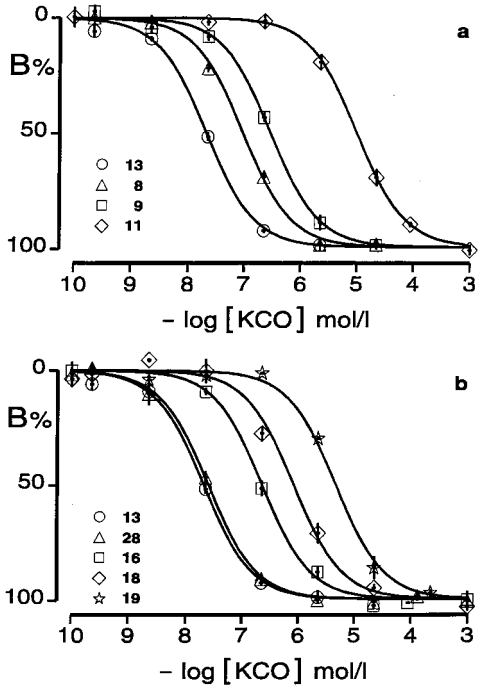

Figure 2. Impact of sulfonamide variation on binding affinities in myocardial membranes. Both exchanging phenyl (**13**) by alkyl (**8**, **9**, and **11**), shown in part a, and substitution of phenyl in the ortho and para positions (**16**, **18**, and **19**), shown in part b, result in a severe loss of activity, whereas replacement of the spacer −NH− by −O− retains affinity. Dissociation constants (pK_D) estimated by nonlinear regression of nonnormalized data are listed in Table 1.

Tertiary aliphatic sulfonamides **21**−**23** exhibit no advantage for affinity in comparison to the secondary analogues **8** and **9**. The tertiary aromatic sulfonamide **24**, however, representing the N-methylation product of **13**, almost retains the high affinity of the latter.

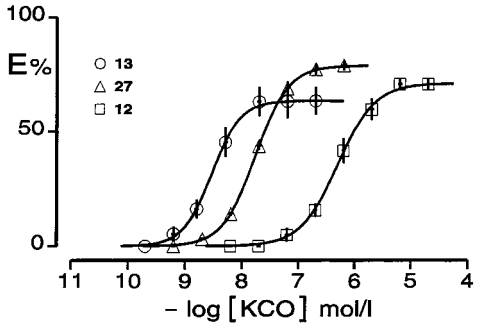

Figure 3. Relaxation of isolated rings of rat aorta, precontracted by 25 mM KCl. Dependence of ligand affinity on the spacer length between the chromene and the phenyl ring is shown. Elongation of the spacer by including a methylene group (**12**) decreases affinity by about 2 orders of magnitude, compared to **13**. Shortening of the linker by depletion of the amino group (**27**) decreases affinity by a factor of about 8. Isolated rings of rat aorta were dose-dependently relaxed by the indicated concentrations of compounds **13**, **27**, and **12**. Maximum effects calculated as a percentage of basal tension before addition of KCl were significantly smaller than 100%.

Inspecting the data for aortic relaxation in Table 2 reveals that five test compounds (**5**, **13**, **14**, **24**, and **28**) surpass bimakalim in dilator potency. The high potency of **5** nicely fits the findings of a previous study[22] in which 6-fluorosulfonyloxy substitution resulted in the compound with the highest vasodilator potency. **24** is the most active KCO of the 4-pyridonechromenes published so far. The impact of adequate positioning of the phenyl ring is substantiated in Figure 3. If the distance of the phenyl ring to the chromene nucleus is either too long (**12**) or too short (**27**), there is a significant reduction of dilator activity.

Kinetics of aortic relaxation by sulfonamide derivatives are markedly retarded compared to the remaining compounds. A representative experiment is depicted in Figure 4, demonstrating that equal concentrations (30 nmol/L) of equipotent compounds, the sulfonamide **13** and the sulfonyloxy derivative **28**, exhibit slow and fast kinetics, respectively. Half-times for relaxation ($n = 4$) were 3.8 ± 0.2 min for **28** and 10.5 ± 0.5 min for **13**, resulting in an approximately 3-fold increase of half-time.

The retardation of relaxation could be caused by a retarded association of **13** with its binding site at the K_{ATP}-channel and/or by a slow drug access, i.e., a slow diffusion of **13** via the plasmalemma to reach its intracellular binding site. The feasibility of experiments to measure association rates of drug-receptor complexes appears limited unless a radiolabeled derivative of **13** is available. However, the second hypothesis, the slowdown of drug access of **13** versus **28**, appears promising because it is well-known that amides generally exhibit stronger nonspecific protein binding than esters. Thus, it is likely that physicochemical parameters are responsible for a slowdown of drug diffusion into the aortic tissue or for a retarded passage through the plasmalemma resulting in a retarded occupation of intracellular binding sites. It remains to be clarified whether the retardation of the drug effect, as observed for **13**, could represent a therapeutic target, as an alternative to the prodrug approach, to achieve a slow onset of the in vivo action to prevent side effects such as tachycardia.[23]

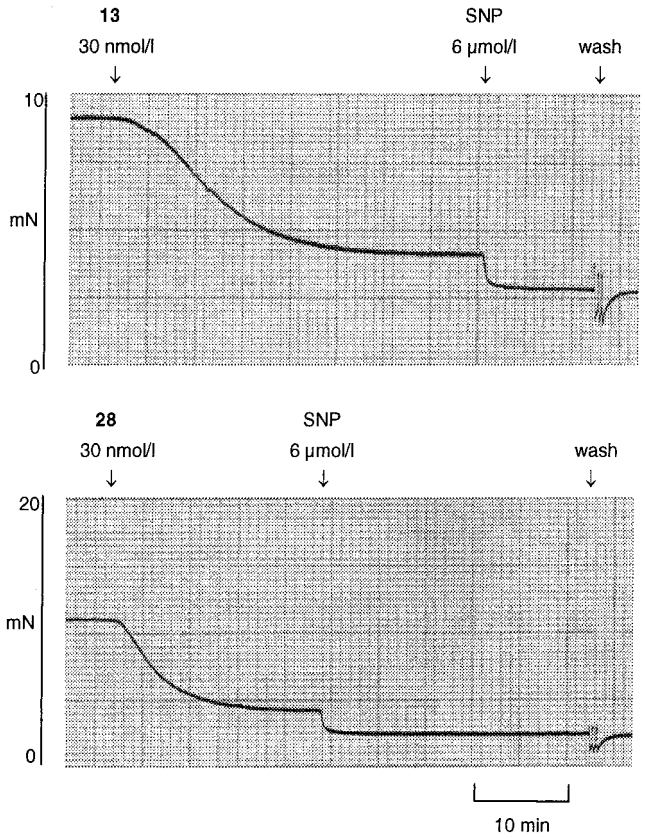

Figure 4. Relaxation kinetics of compounds **13** and **28** in rat aortic rings. Details are given in section B of the Experimental Section. Relaxation was induced with 30 nM of **13** and **28**. Concentrations were chosen to induce approximately 90% of maximum relaxation achievable by KCOs. Complete relaxation was observed in the presence of 6 μM sodium nitroprusside (SNP). Half-times of relaxation by **13** and **28** were 10.0 and 3.5 min, respectively.

To evaluate our set of compounds in a further biological test system, we used rat tracheal strips. The results are summarized in Table 2. The ranking in potency is rather parallel to that in aorta. Absolute values of pEC_{50} always indicate higher activities in the aorta. In both test systems the KCOs exhibit potency ranges of roughly 3 log units: in rat aorta from a pEC_{50} value of 8.76 for the 6-*N*-phenyl-*N*-methylsulfonamido derivative **24** to 5.68 for the *N*-*p*-nitrophenylsulfonamido derivative **20**; in rat trachea from a pEC_{50} value of 8.01 to 4.99 for the same compounds. The differences between the pEC_{50} values are given as $\triangle pEC_{50}$ in Table 2, ranging from 0.40 for compound **12** to 1.30 for compound **5**.

Beyond the absolute affinity values, a selective binding of KCOs to the different types of K_{ATP}-channels of different organs is one of the most demanding challenges in K_{ATP}-channel research. On the basis of the successful cloning of inwardly rectifying K^+ channels (KIR) and of sulfonylurea receptors (SUR), it is widely accepted that the SUR subtypes SUR1, SUR2A, and SUR2B are responsible for the differential effects of KCOs on each type of K_{ATP}-channels.[24] For instance, pinacidil activates channels composed of Kir6.2 as an inwardly rectifying K^+ channel subunit with SUR2A or SUR2B but not with SUR1. In contrast, diazoxide activates channels composed of Kir6.2 with SUR1 and SUR2B but not with SUR2A. Further evidence indicating differences in SUR2A and SUR2B was published by

Quast and co-workers.[25] Kinetic experiments revealed a faster dissociation of the [^{3}H]-P 1075/SUR2A complex compared to SUR2B, resulting in a 7-fold higher overall affinity of P 1075 to SUR2B. Competition binding experiments resulting in approximately 4 times lower affinities of KCOs for SUR2A were in the same line, whereas the antagonist glibenclamide exhibited an 8-fold higher affinity in favor of SUR2A.

From these findings it may be assumed that compounds could be found that discriminate at least between cardiac (presumably composed of SUR2A/Kir6.2) and smooth muscle (presumably composed of SUR2B/Kir6.1) K_{ATP}-channels or that even discriminate between different types of smooth muscle, e.g., between arterial and bronchial smooth muscle. Targeting this open question, we investigated the new 6-sulfonylchromenes in functional and binding assays. To test the influence of different methods, we first compared functional data of rat aorta with binding data measured in cultivated rat aortic smooth muscle cells. The correlation of pEC_{50} values for aortic relaxation (Table 2) and pK_D values for binding (Table 1) in cultivated smooth muscle cells (SMC) is characterized by the following equation:

$$pEC_{50}(\text{aorta}) = (0.934 \pm 0.077)(pK_D(\text{SMC})) + (0.875 \pm 0.550) \quad (1)$$

$$n = 19; \quad r = 0.947; \quad s = 0.310; \quad F = 148$$

However, despite the significant correlation, it became evident that EC_{50} concentrations were on average 6-fold (~0.77 log units) lower than pK_D values; this systematic deviation had also been described by Quast et al.[26] comparing binding and relaxation in rat aortic rings.

Because of this systematic deviation, we restricted the further analyses of hypothetical selectivities to comparisons of data obtained with the same experimental method. By comparison of the relaxation of aortas and tracheas, both characterized by EC_{50} values, again a nice correlation was found:

$$pEC_{50}(\text{aorta}) = (1.056 \pm 0.055)(pEC_{50}(\text{trachea})) + (0.441 \pm 0.368) \quad (2)$$

$$n = 21; \quad r = 0.975; \quad s = 0.219; \quad F = 369$$

Interestingly, aortic relaxation occurred with 5- to 8-fold ($\Delta \log = 0.81 \pm 0.05$) lower concentrations of KCOs than tracheal relaxation, indicating a vasoselectivity of KCOs. The smallest differences (see Table 2) of about half a log unit were observed with compounds **7**, **11**, and **12** characterized by aliphatic residues; differences of more than 1 log unit were found with compounds **5** and **6** characterized by very small substituents ($-F$, $-N_3$). However, before selectivities of compounds for arterial versus tracheal K_{ATP}-channels are postulated, it should be considered that different contracture models (25 mmol/L K^+ in aorta, 0.6 μM carbachol in trachea) were used to study the relaxation by KCOs.

Whereas in the aorta K^+ concentrations lower than 30 mmol/L allow recordings of highly efficient effects by KCOs, in trachea the muscarinic (M_2/M_3 receptor) agonist carbachol exerts functional antagonistic effects against an effective relaxation by KCOs. These antagonistic effects result in a shift of EC_{50} values for relaxation by KCOs toward higher concentrations. The extent of the antagonistic effect may be extrapolated from a comparison of relaxation by rilmakalim of tracheas precontracted with 0.2 and 2.0 μM carbachol (unpublished observations). EC_{50} values ($-\log$, M) for rilmakalim were 7.84 ± 0.02 and 7.30 ± 0.03 in the presence of 0.2 and 2 μM carbachol, respectively, resulting in a difference of ~0.5 log units. From this finding it may be extrapolated that EC_{50} values for relaxation by KCOs of tracheas under the hypothetical condition of spontaneous tone (i.e., complete absence of carbachol) are to be observed with 3-fold (0.5 log units) lower concentrations as observed in the presence of 0.6 μM carbachol. Thereby, the mean difference of aortic and tracheal relaxation of 0.81 ($\Delta \log$, M) is reduced to a negligible amount, indicating that hypothetical differences between aortic and tracheal K_{ATP}-channels cannot be detected with the synthesized set of compounds.

Alternative hypotheses to explain the putative vasoselectivity might be based on differences of receptor densities in vasal and tracheal smooth muscle cells. However, preliminary experiments in cultured smooth muscle cells of calf coronary arteries[27] and of enzymatically isolated smooth muscle cells of calf tracheas[28] assayed with [^{3}H]-P 1075 as radioligand hint at similar densities of about 10 000−30 000 K_{ATP}-channels per cell for both tissues.

On the basis of the findings of different affinities of ligands for SUR2A and SUR2B cited above, it was expected that differences in affinities of the synthesized compounds could occur in cardiac and smooth muscle cells. Therefore, binding experiments were performed in cultivated smooth muscle cells of rat aorta and in purified membrane particles of rat heart. However, a comparison of K_D data again revealed a highly significant correlation,

$$pK_D(\text{heart}) = (0.950 \pm 0.058)(pK_D(\text{SMC})) + (0.054 \pm 0.414) \quad (3)$$

$$n = 24; \quad r = 0.962; \quad s = 0.247; \quad F = 270$$

hinting at a large similarity of structural properties of K_{ATP}-channels of heart myocytes and aorta smooth muscle cells with respect to the analyzed set of compounds.

Affinity differences (ΔpK_D values in Table 1) in heart myocytes and aortic smooth muscle cells were small but significantly different from zero with a mean ΔpK_D of 0.41 ± 0.05, indicating that affinities in aortic smooth muscle cells are on average 2- to 3-fold higher than in aortic smooth muscle cells. This small difference of affinities of a set benzopyran derivatives matches a 4-fold difference in affinity of a set of seven chemically diverse KCO[25] measured with radioligand binding in HEK 293 cells expressing SUR2A and SUR2B.

From this point of view, it may be concluded that the differences between SUR2A and SUR2B, which were found to be splice variants differing only within the last 42 amino acids of the carboxyl terminus,[2,16] are not relevant for binding of the analyzed set of chromene analogues. This interpretation is in line with molecular biological findings based on the exchange of domains between SUR1 and SUR2B[17] such that binding sites on the transmembrane domain II are critical for KCO binding. Recently, however, it was reported that not only

the molecular structure of transmembrane domain II but also the coupling of the pore-forming subunits of the Kir6.*x* family to the sulfonylurea receptor subtypes may influence the binding potency of KCO.[29] Thus, we feel that the discovery of subtype-selective ligands remains an open question.

On the basis of the biological data, we used chemometric approaches to derive QSAR models. In the absence of knowledge about the preferred bioactive conformation of our test molecules, we applied the alignment-independent approach GRIND (*gr*id *in*dependent *d*escriptors). GRIND are briefly explained in the Experimental Section; an extensive report is given by Pastor et al.[30] Three probes were used: the DRY probe for describing hydrophobic receptor interactions, the carbonyl oxygen (O probe) to define hydrogen-bond-accepting regions, and the amide nitrogen (N1 probe) to define hydrogen-bond-donating receptor regions. When these three probes were applied, 246 descriptors were derived. When PLS analysis was used, no significant correlation between vasodilator activity in aorta and chemical descriptors could be detected. In the case of three components, a rather low correlation coefficient, r, of 0.706 and a rather high standard deviation of the error of calculation, SDEC, of 0.651 were obtained. For a five-component model the corresponding values are $r = 0.762$ and SDEC = 0.596. Cross-validation of the models using the LOO (leave-one-out) technique underlines the poor quality of the above models and yields no significant q^2 values. The strongest outliers in the PLS analysis are **13** and **24** (underestimated) as well as **11** (overestimated).

The high binding affinity and strong dilator potency of compound **13**, representing a pronounced outlier in the QSAR model, led us to analyze its conformational behavior in more detail.[31] First of all, we investigated the crystal structure of **13** by means of X-ray analysis (Figure 5a). The analysis of the structure parameters clearly indicates the existence of four centers of association of the single molecule: intermolecular H-bonding between sulfonyl-NH and pyridone-carbonyl moieties documents the H bridging donor and acceptor capability of the molecule (Figure 5b). Pyridone and *N*-phenyl rings are involved in π-stacking,[32] clearly indicating additional association properties (Figure 5c). The planes of the pyridone and the chromene moiety are forced into an orthogonal position in the crystal. The *N*-phenyl ring takes a strongly wrinkled position in relation to the chromene, resulting in a slightly distorted, quasi-parallel orientation with respect to the pyridone nucleus.

To clarify, whether the solid-state conformation is also predominant in solution, the ^{1}H NMR spectra of **13** and several selected sulfonamide derivatives were thoroughly investigated in comparison to the 6-H derivative **3**. Introduction of 6-sulfonamide substituents results in a characteristic influence on the aromatic protons of the chromene ring (H-5, H-7, and H-8), which are paramagnetically shifted to a different extent (Table 4). In the case of aliphatic sulfonamides, this low-field shift ($\Delta\delta$), measured in the solvent $CDCl_3$, almost equivalently influences the two ortho-positioned protons H-5 and H-7. In contrast, the paramagnetic shift of H-5 is twice that of H-7 when the aromatic sulfonamides **13**, **18**, and **24** are investigated. This finding might be due to steric

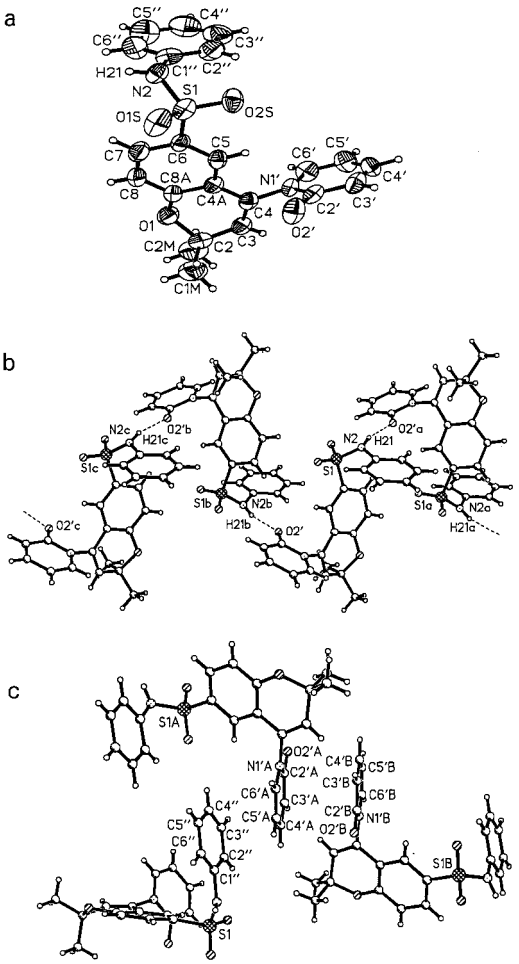

Figure 5. X-ray structure of **13**. (a) Diagram of a single molecule in a crystal of **13** showing the atom labeling. Displacement ellipsoids are drawn at the 50% probability level, radii of hydrogen atoms are chosen arbitrarily, and the hydrogen atom labels are omitted for clarity. (b) Solid-state interaction by N−H···O hydrogen bonding linking the single molecules to supramolecular chains. Symmetry codes are the following: a, $0.5 - x, -0.5 + y, 0.5 - z$; b, $0.5 - x, 0.5 + y, 0.5 - z$; c, $x, 1 + y, z$. (c) π-Stacking interactions of *N*-phenyl groups and pyridone moieties demonstrating further association capabilities of the compound. Between the phenyl group and the pyridone group, the more attractive slipped type of $\pi-\pi$ interaction is found. Symmetry codes are the following: A, $1.5 - x, -0.5 + y, 0.5 - z$; B, $0.5 + x, -0.5 - y, -0.5 + z$.

interactions resulting from a restricted rotation of the entire 6-substituent around the bond to the benzopyran ring. Thereby, H-7 could be shielded by the anisotropic effect of the aromatic ring current more than H-5.

To explain these findings, we measured ^{1}H NMR spectra of the deuterated compound **14** at 500 MHz. The absence of the phenyl protons allows the unequivocal localization of the remaining aromatic protons. Thus, the influence of different solvents and temperature-dependent effects could be investigated more precisely. To our great surprise, the anisotropic effect of the 6-substituent observed in $CDCl_3$ could not be detected in deuterated methanol. The two ortho-positioned protons H-5 and H-7 are identically influenced under these conditions. Cooling the methanolic solution to −60 °C does not modify the above observations (Table 5). Under the latter conditions, only the protons of the pyridone moiety (in particular H-6′) exhibit a significant para-

Table 3. Chemical Data of Sulfonamides **8**−**23** and **29**

compd	yield, %	preparation method	mp, °C	recryst solvent	formula (M_r)
8	73	a	173	acetone/hexane	$C_{17}H_{18}N_2O_4S$ (346.41)
9	54	a	88	toluene/ether/hexane	$C_{18}H_{20}N_2O_4S$ (360.43)
10	42	a	185	acetone/hexane	$C_{18}H_{20}N_2O_5S\cdot 0.5H_2O$ (385.44)
11	47	a	237	acetone/hexane	$C_{19}H_{22}NO_4S$ (374.46)
12	41	a	193	toluene/ether/hexane	$C_{23}H_{22}N_2O_4S$ (422.50)
13	75	b	249	2-propanol	$C_{22}H_{20}N_2O_4S$ (408.48)
14	67	b	249	2-propanol	$C_{22}H_{15}D_5N_2O_4S$ (413.52)
15	28	b	173	acetone/hexane	$C_{22}H_{19}FN_2O_4S$ (426.47)
16	31	b	173	ether/hexane	$C_{22}H_{20}BrN_2O_4S$ (488.38)
17	36	b	116	CH_2Cl_2/hexane	$C_{22}H_{20}BrN_2O_4S$ (488.38)
18	53	b	210	CH_2Cl_2/hexane	$C_{23}H_{22}N_2O_5S$ (438.50)
19	37	c	258	acetone/hexane	$C_{23}H_{19}N_3O_4S$ (433.49)
20	34	c	281	acetone/hexane	$C_{22}H_{19}N_3O_6S$ (453.47)
21	81	a	234	acetone/hexane	$C_{18}H_{20}N_2O_4S$ (360.43)
22	71	a	136	acetone/hexane	$C_{20}H_{24}N_2O_4S$ (388.49)
23	63	a	124	acetone/hexane	$C_{20}H_{22}N_2O_5S$ (402.47)
29	43	a	155	CH_2Cl_2/hexane	$C_{21}H_{24}N_2O_4S$ (400.50)

Table 4. Chemical Shifts of Aromatic Protons of the Chromene Ring of Selected Sulfonamides

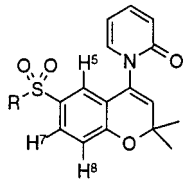

	R	δ H-5[a]	Δδ[b]	δ H-7[a]	Δδ[b]	δ H-8[a]	Δδ[b]
		Aliphatic Sulfonamides					
7	NH_2	7.22	+0.56	7.72	+0.56	6.93	+0.13
8	NH−CH_3	7.16	+0.50	7.66	+0.50	6.94	+0.14
11	NH−$CH(CH_3)_2$	7.17	+0.51	7.68	+0.52	6.93	+0.13
21	N−$(CH_3)_2$	7.07	+0.41	7.59	+0.43	6.96	+0.16
22	N−$(CH_2$−$CH_3)_2$	7.09	+0.43	7.62	+0.46	6.92	+0.12
		Aromatic Sulfonamides					
13	NH−Ph	7.09	+0.43	7.41	+0.25	6.77	−0.03
18	NH−*p*-OCH_3−Ph	7.09	+0.43	7.37	+0.21	6.77	−0.03
24	N−(CH_3)−Ph	6.91	+0.25	7.31	+0.15	6.85	+0.05

[a] Chemical shift δ in ppm. [b] Paramagnetic/diamagnetic shift compared to the 6-H derivative **3**. All spectra were measured in $CDCl_3$ at 200 MHz.

magnetic shift, which is presumably due to the stabilization of a dipolar zwitterionic structure in deuterated methanol (Scheme 4). The same behavior is observed with 1-methyl-2-pyridone. With regard to an interpretation of structure−activity relationships, these findings indicate that the 6-phenylsulfonamide substituent in **13** and **14** is quite flexible and exhibits not necessarily a preferred orientation, like this is given, for instance, in the crystal structure and in the solvate complex with $CDCl_3$.

Table 5. Influence of Solvent and Temperature on the ^1H Chemical Shifts of **14**

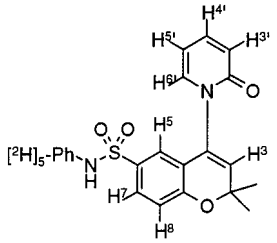

solvent	δ H-5[a]	Δδ[b]	δ H-7[a]	Δδ[b]	δ H-8[a]	Δδ[b]
$CDCl_3$	7.09	+0.43	7.41	+0.25	6.77	−0.03
CD_3OD	6.91	+0.36	7.52	+0.35	6.86	+ 0.03

proton	δ (30 °C)[c]	δ (0 °C)[c]	δ (−20 °C)[c]	δ (−40 °C)[c]	δ (−60 °C)[c]	Δδ [d]
H-3	5.96	6.00	6.02	6.05	6.07	+0.11
H-5	6.91	6.89	6.90	6.91	6.93	−0.02
H-7	7.52	7.52	7.51	7.51	7.52	±0.00
H-8	6.86	6.86	6.86	6.86	6.86	±0.00
H-3′	6.62	6.64	6.65	6.67	6.68	+0.06
H-4′	7.66	7.70	7.72	7.75	7.77	+0.11
H-5′	6.48	6.52	6.55	6.57	6.60	+0.12
H-6′	7.38	7.45	7.51	7.55	7.61	+0.23

[a] Chemical shift δ in ppm. [b] Paramagnetic/diamagnetic shift compared to the 6-H derivative **3**. Spectra in CD_3OD were recorded at 500 MHz. [c] Chemical shift δ in ppm (CD_3OD, 500 MHz) at given temperature. [d] Difference between δ measured at 60 °C and δ measured at 30 °C.

Scheme 4

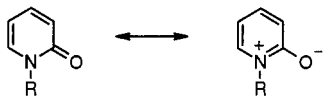

The remaining two highly potent compounds **24** and **28** are not capable of H-bonding interactions because of a missing NH group. Therefore, the phenyl moieties of the corresponding 6-substituents in **24** and **28** can readily adopt conformations, which resemble the spatial orientation in **13** and **14**.

It is possible that these rather flexible 6-substituents are able to reach an additional interacting region within the receptor area for chromene KCOs. Correspondingly, we assume that the receptor area exhibits two separate interaction sites with the capacity to bind the 6-substituent of the chromenes: (a) one site interacting with the negatively polarized partial structure (e.g., CN, NO_2, SO_2), and (b) one spatially restricted site enabling favorable π-interactions,[33,34] as also shown in X-ray studies.

The hypothetical interaction site mentioned in item b might explain why larger aliphatic substituents of the sulfonamido N (**11** or **12**) induce dramatic diminutions of biological activity. This was finally confirmed by the aid of the 6-cyclopentylsulfonamido derivative **29**, the structure of which is almost identical to that of **13**, lacking only the capacity of π-interactions. **29** was subsequently synthesized and showed only rather poor binding affinity (see Table 1).

Conclusion

Compounds **13**, **24**, and **28** represent the most potent KCOs of the 4-pyridonechromene type published so far. A major outcome of our investigations is the delineation of a second binding pocket at the K_{ATP}-channel receptor

in addition to that already known. Apparently a second site seems to be present that enables favorable π-interactions. This might open routes to the exploration of new and highly wanted tissue-selective KCOs.

Experimental Section

A. Chemistry. Melting points were taken on a Reichert Thermovar microscope and are uncorrected. ^{1}H NMR spectra were recorded on a Bruker AC-200 or AC-500 spectrometer. IR spectra were measured on a Perkin-Elmer 1600 FT-IR spectrometer. MS spectra were recorded on a Finnigan MAT 4000 spectrometer (EI, 70 eV) or an INCOS 50 Finnigan MAT (DCI, NH_3). Elemental analyses (C, H, N) were carried out in the microanalytical center (Heinrich-Heine-Universität Düsseldorf) with a Perkin-Elmer PE2400 CHN elemental analyzer and were within ±0.4% of the calculated values. Solvents were all of anhydrous grade and were obtained from commercial suppliers.

6-Chlorosulfonyl-4-(1,2-dihydro-2-oxo-1-pyridyl)-2,2-dimethyl-2*H*-1-benzopyran (4). The benzopyran **3**[22] (253 mg, 1 mmol) was dissolved in 5 mL of chloroform, and the solution was chilled to −15 °C (crushed ice/NaCl). A solution of 1 mL of chlorosulfonic acid in 10 mL of chloroform was added under stirring over a period of 0.5 h. During this time the temperature should not rise above −10 °C. After the mixture was further stirred at room temperature (0.5 h), the reaction was finished by addition of crushed ice. After separation of the organic phase, the aqueous solution was extracted with chloroform. The organic layer was dried ($MgSO_4$) and evaporated. The residue was recrystallized from acetone/hexane to give **4** as colorless needles (273 mg, 78%): mp 186 °C; ^{1}H NMR ($CDCl_3$) δ 1.60 (s, 3H), 1.66 (s, 3H), 5.86 (s, 1H), 6.31 ("dt", 1H), 6.68 ("d", 1H), 7.01 (d, J = 9.1 Hz, 1H), 7.17 ("dd", 1H), 7.30 (d, J = 2.2 Hz, 1H), 7.48 (m, 1H), 7.85 (dd, J = 9.1 and 2.2 Hz, 1H); IR (KBr) 1666, 1588, 1531, 1375, 1286, 1177, 1140, cm^{-1}; MS (EI) 351 (31, M), 338 (37), 336 (100), 259 (20), 257 (51), 237 (33), 168 (18), 159 (23), 154 (22), 128 (21), 78 (47). Anal. ($C_{16}H_{14}ClNO_4S$) C, H, N.

6-Fluorosulfonyl-4-(1,2-dihydro-2-oxo-1-pyridyl)-2,2-dimethyl-2*H*-1-benzopyran (5). The sulfonyl chloride **4** (106 mg, 0.3 mmol) was refluxed in 10 mL of a 73% aqueous KF solution for 1 h.[35] After the mixture was cooled to room temperature, the precipitate was filtered, washed with cold water, and recrystallized from water/ethanol to give white crystals of **5** (77 mg, 77%): mp 183 °C; ^{1}H NMR ($CDCl_3$) δ 1.59 (s, 3H), 1.66 (s, 3H), 5.86 (s, 1H), 6.30 ("dt", 1H), 6.67 ("d", 1H), 7.03 (d, J = 8.6 Hz, 1H), 7.17 ("dd", 1H), 7.27 (d, J = 2.1 Hz, 1H), 7.47 (m, 1H), 7.81 (dd, J = 8.6 and 2.1 Hz, 1H); IR (KBr) 1670, 1594, 1405, 1202, 1141 cm^{-1}; MS (EI) 335 (10, M), 320 (34), 241 (24), 95 (22), 78 (100). Anal. ($C_{16}H_{14}FNO_4S$) C, H, N.

6-Azidosulfonyl-4-(1,2-dihydro-2-oxo-1-pyridyl)-2,2-dimethyl-2*H*-1-benzopyran (6). A saturated solution of NaN_3 in water (5 mL) was diluted with 10 mL of ethanol and filtered.[36] Sulfonyl chloride **4** (106 mg, 0.3 mmol) was dissolved in a minimum amount of ethanol and was mixed with the azide solution. After some time a solid separated, and dropwise addition of water forced this process. The precipitate was filtered, washed with cold water, and dried in vacuo to give a white powder of **6** (52 mg, 48%): mp 174 °C; ^{1}H NMR ($CDCl_3$) δ 1.59 (s, 3H), 1.65 (s, 3H), 5.85 (s, 1H), 6.28 ("dt", 1H), 6.66 ("d", 1H), 7.01 (d, J = 8.6 Hz, 1H), 7.16 ("dd", 1H), 7.22 (d, J = 2.1 Hz, 1H), 7.46 (m, 1H), 7.76 (dd, J = 8.6 and 2.1 Hz, 1H); IR (KBr) 2119, 1668, 1593, 1533, 1374, 1287, 1176, 1157, 1140, 1081 cm^{-1}; MS (EI) 358 (19, M), 343 (11), 317 (26), 268 (19), 263 (26), 251 (53), 237 (51), 223 (21), 208 (32), 157 (32), 126 (76), 112 (58), 103 (49), 96 (73), 77 (100). Anal. ($C_{16}H_{14}N_4O_4S$) C, H, N.

6-Aminosulfonyl-4-(1,2-dihydro-2-oxo-1-pyridyl)-2,2-dimethyl-2-*H*-1-benzopyran (7). Sulfonyl chloride **4** (352 mg, 1 mmol) was dissolved in 20 mL of 1,4-dioxane. This solution was heated to 60 °C while a constant stream of NH_3 was passed through. After 1 h, the reaction was interrupted and the solution was diluted with 100 mL of water, acidified with dilute sulfuric acid, and extracted with dichloromethane. The organic layer was washed with water, dried ($MgSO_4$), and evaporated. The residue was recrystallized from acetone/hexane to give **7** as white needles (212 mg, 64%): mp 216 °C; ^{1}H NMR ($CDCl_3$) δ 1.56 (s, 3 H), 1.62 (s, 3H), 4.90 (s, 2H), 5.79 (s, 1H), 6.29 ("dt", 1H), 6.36 ("d", 1H), 6.93 (d, J = 8.6 Hz, 1H), 7.18 ("dd", 1H), 7.22 (d, 1H), 7.47 (m, 1H), 7.72 (dd, J = 8.6, 1H); IR (KBr) 1659, 1583, 1534, 1338, 1278, 1168, 1150 cm^{-1}; MS (EI) 332 (10,M), 317 (35), 238 (31) 96 (100), 78 (50), 51 (19). Anal. ($C_{16}H_{16}N_2O_4S$) C, H, N.

General Procedures for the Syntheses of Sulfonamides. Method a for Preparation of Aliphatic Sulfonamides 8−12, 21−23, and 29. The sulfonyl chloride **4** (176 mg, 0.5 mmol) was triturated with 1.5 mmol of the corresponding amine (methyl- and ethylamine were used as 40% and 70% aqueous solutions, respectively). The resulting suspensions were diluted dropwise with 1,4-dioxane to a homogeneous paste. After 0.5 h of standing at room temperature, the reaction mixtures were diluted with 50 mL of sulfuric acid (2%) and extracted with dichloromethane. These extracts were dried immediately ($MgSO_4$) and evaporated. Each residue was recrystallized as described in Table 3.

Method b for Preparation of Aromatic Sulfonamides 13−18. The sulfonyl chloride **4** (176 mg, 0.5 mmol) was triturated with 1 mmol of the corresponding aromatic amine and an additional 1 mL of triethylamine at room temperature. Each suspension was dropwise diluted with 1,4-dioxane to a homogeneous paste or solution. After 1 h at room temperature, each reaction mixture was diluted with 50 mL of sulfuric acid (10%) and extracted with dichloromethane. The organic layers were washed with water, dried ($MgSO_4$), and evaporated. Recrystallization as described in Table 3 afforded the analytically pure compounds.

Method c for Preparation of Sulfonamides 19 and 20. The sulfonyl chloride **4** (176 mg, 0.5 mmol) was homogeneously triturated with 4-aminobenzonitrile (118 mg, 1 mmol), and the mixture was fused in an oil bath at 85 °C for 15 min. Alternatively, 4-nitroaniline (138 mg, 1 mmol) was melted with **4** (176 mg, 1 mmol) at 180 °C for 15 min. After cooling, each reaction mixture was taken up in 50 mL of dichloromethane. The organic phase was successively washed with 10% sulfuric acid to remove excess aniline and water and was dried ($MgSO_4$). After evaporation, the residues were recrystallized as shown in Table 3.

4-(1,2-Dihydro-2-oxo-1-pyridyl)-2,2-dimethyl-6-(*N*-methyl-*N*-phenylaminosulfonyl)-2*H*-1-benzopyran (24). Compound **13** (204 mg, 0.5 mmol) was dissolved in a mixture of 6 mL of 0.1 NaOH and 4 mL of ethanol. After addition of 1 mL of methyl iodide, the mixture was heated for 1 h (reflux condenser). After cooling and addition of 30 mL of water, the solution was acidified with dilute sulfuric acid and extracted with ether. The organic layer was washed with water, dried ($MgSO_4$), and evaporated. The remaining residue was recrystallized from 2-propanol to give **24** as white needles (131 mg, 62%): mp 184 °C; ^{1}H NMR ($CDCl_3$) δ 1.53 (s, 3H), 1.64 (s, 3H), 3.10 (s, 3H), 5.78 (s, 1H), 6.21 ("dt", 1H), 6.56 ("d", 1H), 6.85 (d, 1H), 6.91 (d, 1H), 7.1 (m, 3 H), 7.2−7.8 (m, 5H); IR (KBr) 1667, 1590, 1530, 1350, 1275, 1174, 1147, 707 cm^{-1}; MS (EI) 422 (4, M), 407 (20), 253 (100), 237 (49), 128 (21), 106 (38), 96 (34), 78 (39). Anal. ($C_{23}H_{22}N_2O_4S$) C, H, N.

General Procedure for the Synthesis of Sulfonylureas 25 and 26. According to the procedure of Petersen,[37] compound **7** was suspended in a mixture of 3 mL of acetone and 10 mL of 0.05 N NaOH. A solution of the corresponding isocyanate (1 mmol in 3 mL of acetone) was added drop by drop under continuous stirring at room temperature. After 0.5 h the mixture was filtered, and the filtrate was carefully acidified with acetic acid. The resulting precipitate was filtered off, washed with water, and dried. This crude material was further purified by silica gel chromatography with toluene/acetone (70/30).

4-(1,2-Dihydro-2-oxo-1-pyridyl)-2,2-dimethyl-6-(phenylaminocarbonylaminosulfonyl)-2*H*-1-benzopyran (25).

White crystals (36 mg, 16%); mp 201 °C (from acetone/hexane); ^{1}H NMR (DMSO-d_6) δ 1.51 (s, 3H), 1.54 (s, 3H), 6.13 (s, 1H), 6.37 ("dt", 1H), 6.50 ("d", 1H), 7.0−7.1 (m, 3H), 7.2−7.4 (m, 4 H), 7.5−7.6 (m, 2H), 7.81 (dd, J = 8.6 and 2.1 Hz, 1H), 8.76 (s, 1H), 10.66 (s, 1H); IR (KBr) 1724, 1655, 1600, 1569, 1535, 1148 cm^{-1}; MS (EI) 358 (2, M − 93), 343 (8), 332 (7), 317 (25), 238 (38), 157 (27), 119 (88), 96 (92), 93 (77), 91 (56), 78 (100). Anal. ($C_{23}H_{21}N_3O_5S$) C, H, N.

6-(Cyclohexylaminocarbonylaminosulfonyl)-4-(1,2-dihydro-2-oxo-1-pyridyl)-2,2-dimethyl-2*H*-1-benzopyran (26). White crystals (30 mg, 13%); mp 148 °C (dec) from acetone/hexane; ^{1}H NMR ($CDCl_3$) δ 0.95−1.40 (m, 5H), 1.55−1.85 (m, 5H), 1.57 (s, 3H), 1.63 (s, 3H), 3.4−3.5 (m, 1H), 5.81 (s, 1H), 6.18 ("d", 1H), 6.31 ("d", 1H), 6.94 (d, J = 8.6 Hz, 1H), 7.1−7.2 (m, 2H), 7.47 (m, 1H), 7.77 (dd, J = 8.6 Hz, 1H); IR (KBr) 1706, 1661, 1573, 1535, 1343, 1276, 1167, 1149 cm^{-1}; MS (EI) 332 (6, M − 125), 317 (17), 238 (15), 96 (45), 56 (62), 44 (100); MS (DCI) 475 (100, M + NH_4), 458 (22, M + H), 376 (39), 350 (58). Anal. ($C_{23}H_{27}N_3O_5S\cdot0.5H_2O$) C, H, N.

4-(1,2-Dihydro-2-oxo-1-pyridyl)-2,2-dimethyl-6-phenylsulfonyl-2*H*-1-benzopyran (27). A solution of sulfonyl chloride **4** (352 mg, 1 mmol) in 20 mL of dry benzene was added to dry $AlCl_3$ (335 mg, 2.5 mmol). This mixture was stirred at room temperature (1 h) and then poured onto dilute HCl. The organic layer was separated, washed with water, and dried. Evaporation gave a solid residue that was recrystallized from acetone/hexane to give **27** as colorless crystals (173 mg, 44%): mp 82 °C; ^{1}H NMR ($CDCl_3$) δ 1.55 (s, 3H), 1.59 (s, 3H), 5.79 (s, 1H), 6.28 ("dt", 1H), 6.66 ("d", 1H), 6.91 (d, J = 8.6 Hz, 1H), 7.15 ("dd", 1H), 7.30 (d, 1H), 7.42−7.54 (m, 4H), 7.68 (dd, J = 8.6 Hz, 1H), 7.8−7.9 (m, 2H); IR (KBr) 1670, 1595, 1277, 1162, 1148, 1089 cm^{-1}; MS (EI) 393 (5, M), 378 (20), 299 (16), 128 (13), 115 (16), 96 (17), 78 (100). Anal. ($C_{22}H_{19}NO_4S$) C, H, N.

4-(1,2-Dihydro-2-oxo-1-pyridyl)-2,2-dimethyl-6-phenoxysulfonyl-2*H*-1-benzopyran (28). Phenol (100 mg, 1.06 mmol) was dissolved in 10 mL of dichloromethane, and 5 mL of an aqueous NaOH (30%) and 5 mg of benzyltrimethylammonium bromide were added.[38] To this mixture a solution of the sulfonyl chloride **4** (352 mg, 1 mmol) in 10 mL of dichloromethane was added under vigorous stirring at room temperature, and the mixture was subsequently heated to 40 °C (6 h, reflux condenser). After addition of 30 mL of dichloromethane and 10 mL of water, the organic phase was separated and washed with water. After drying ($MgSO_4$) and evaporation of the organic layer, the residue was recrystallized from dichloromethane/hexane to give **28** as white needles (170 mg, 42%): mp 129 °C; ^{1}H NMR ($CDCl_3$) δ 1.55 (s, 3H), 1.63 (s, 3H), 5.81 (s, 1H), 6.22 ("dt", 1H), 6.60 ("d", 1H), 6.89 (d, J = 8.6 Hz, 1H), 6.97−7.04 (m, 2H), 7.08 ("dd", 1H), 7.14 (d, J = 2.1 Hz, 1H), 7.18−7.35 (m, 3H), 7.41 (m, 1H), 7.56, (dd, J = 8.6 and 2.1 Hz, 1H); IR (KBr) 1666, 1590, 1532, 1483, 1373, 1347, 1279, 1192, 1146, 873, 856, 781, 762 cm^{-1}; MS (EI) 409 (21, M), 394 (37), 315 (29), 268 (28), 252 (45), 237 (97), 221 (19), 158 (43), 157 (41), 128 (58), 115 (26), 96 (100), 78 (80), 65 (21). Anal. ($C_{22}H_{19}NO_5S$) C, H, N.

Crystal Structure Determinations of Compound 13. A crystal of **13** suitable for X-ray study was selected by means of a polarization microscope and was investigated on a Stoe imaging plate diffracton system using graphite-monochromatized Mo Kα radiation (λ = 0.710 73 Å). Unit cell parameters were determined by a least-squares refinement on the positions of 2000 strong reflections distributed equally in reciprocal space. A monoclinic lattice was found, and the space group type $P2_1/n$ was uniquely determined. Crystal data of **13**: M_r-($C_{22}H_{20}N_2O_4S$) = 408.46, a = 8.720(2) Å, b = 12.280(2) Å, c = 19.540(4) Å, β = 100.17°, V = 2059.5(7) Å^3, Z = 4, D_x = 1.317 g cm^{-3}, μ = 0.188 mm^{-1}, T = 293 K, colorless crystal of dimensions 0.11 mm × 0.08 mm × 0.03 mm. A total of 24 121 intensity data points (θ_{min} = 1.97°, θ_{max} = 26.06°) were collected and Lp corrections were applied. The structure was solved by direct methods,[39] and the positions of all hydrogen atoms were found. Refinement (268 parameters including an extinction coefficient χ = 0.0021(2);[40] all of 3967 unique reflections used) by full-matrix least-squares calculations on F^2 [40] converged to the following final indicators: R1[$F_o^2 > 2\sigma(F_o^2)$] = 0.067, wR2 = 0.115 (all data), $w = 1/[\sigma^2(F_o^2) + (0.01P)^2]$ where $P = (F_o^2 + 2F_c^2)/3$, $S = 1.012^{xy}$, $(\Delta/\sigma)_{max} = 0.001$, $\Delta\rho_{max}/\Delta\rho_{min}$ = (0.343 e/Å^2)/(−0.280 e/Å^2). Anisotropic displacement parameters were refined for all non-hydrogen atoms. All H atoms were treated with fixed idealized C−H and N−H distances. The H atoms of the methyl groups were allowed to move collectively around the neighboring C−C axis; for the H atom at nitrogen, allowance was made for variation of the N−H bond direction, and for all the other H atoms, the riding model was applied. The isotropic displacement parameters of the H atoms were kept equal to 120% and 150% of the equivalent isotropic displacement parameters of the parent "aromatic" and primary carbon atom, respectively. Scattering factors, dispersion corrections, and absorption coefficients were taken from International Tables for Crystallography (1992, Vol. C, Tables 6.114, 4.268, and 4.2.4.2).

B. Biological Methods. B.1. Tissue Preparation. Male Wistar rats (body weight 200−300 g) were anesthetized with ether; after opening of the chest, the heart, trachea, and aorta were removed and perfused with modified Krebs solution containing, in mmol/L, 89.0 NaCl, 29.0 $NaHCO_3$, 5.0 KCl, 1.0 Na_2HPO_4, 0.5 $MgSO_4$, 0.04 EDTA, and 2.25 $CaCl_2$ equilibrated with carbogen (95% O_2, 5% CO_2). The water was deionized and doubly distilled in glass. After the removal of connective tissue, fat, and endothelium, aortas were cut into rings of 3 mm width and were mounted in pairs in a modified Blinks apparatus equipped with 7 mL organ baths[41] without further manipulations. Tracheas were opened on the opposite side of the muscle layer, tied on one end to a thread (Flexafil 6/0, J. Pfrimmer and Co., Erlangen, FRG), and also set up in the Blinks apparatus. Each strip was attached to a strain-gauge transducer connected via amplifiers to polygraphs (Watanabe V) for isometric force measurement. In the organ baths the modified Krebs solution was supplemented with, in mmol/L, pyruvate 5, fumarate 5, L-glutamate 5, and glucose 10. The resting force was adjusted to 5 mN (aorta) or 10 mN (trachea) at the beginning of an experiment and remained unchanged throughout the experiment. Experiments were carried out at 32.5 °C.

B.2. Concentration-Effect Curves. At the beginning of each experiment, tissues were allowed to equilibrate in supplemented Krebs solution for 2 h, followed by two successive test contractures at 60 min intervals. In aortic rings test contractures were induced with 25 mmol/L K^+ by replacing 20 mmol/L NaCl by KCl in the Krebs solution described above. In tracheal strips, test contractures were induced with 0.6 μmol/L carbachol. A third contracture was induced to record a cumulative concentration-effect curve for relaxant effects by KCOs. In each experiment eight aortic rings and eight tracheal strips from two animals were investigated simultaneously. Two of the eight preparations served as controls to record the spontaneous changes in tension. Effects (E, %) are expressed as percentages (Δ, %) of basal force (set to 100% relaxation), and maximum force (set to 0% relaxation) was measured before and after induction of contractures. Concentration-effect curves for the test compounds were constructed for each tissue (E, %), and pEC_{50} values were measured by linear extrapolation from half-maximal effect levels to drug concentrations. Means ± SEM of pEC_{50} values and E_{max} values were calculated for n = 4 to n = 6 experiments.

B.3. Relaxation Kinetics for Compounds 13 and 28. Two paired rings of rat aorta were dissected, mounted in two organ baths with a pre-tension of 5 mN, and precontracted with 25 mM KCl. After contractures had reached a stable plateau of tension, relaxation was induced with 30 nM of test compounds. Concentrations were chosen to induce approximately 90% of maximum relaxation achievable by KCOs. Complete relaxation was observed in the presence of 6 μM sodium nitroprusside (SNP). Experiments were terminated by three repetitive changes of the Krebs solution in the organ baths.

B.4. Preparation of Membrane Particles from Rat Heart. Membrane particles were prepared according to Lem-

oine et al.[42] with some modifications. After perfusion with cold Krebs solution and after removal of big vessels, atria, and valves, heart ventricles were minced by scissors and homogenized with a Polytron (PT-12), once at speed 7 for 2 s and twice at speed 3.5 for 20 s. The homogenization buffer was 10 mmol/L TRIS·HCl (pH 7.4) supplemented with 2 mmol/L in the presence of 1 mmol/L EGTA. After dilution (1:20 vol/vol) the homogenate was filtered through japanese silk and centrifuged at 100 g for 10 min. The soft pellet was discarded and the supernatant was collected with 40000 g for 30 min. Pellets were resuspended with 3 mM EGTA/TRIS (pH 7.4) and stored at −80 °C until use.

B.5. Cell Culture of Aortic Myocytes. Aortic myocytes were derived from male wistar rats (200−250 g) by explanting intact rings of rat aortae according to Ross.[43] Aortae were cut into small rings with a width of 1 mm under sterile conditions and explanted in 6-well cell culture dishes (Corning, NY) covered with a thin layer of medium and put into an incubator gassed with 93% O_2 and 7% CO_2. The medium (DMEM, Dulbecco's Modified Eagle's Medium, Gibco, Inchinnan Scotland) was supplemented with 10% fetal calf serum (FCS), 2 mmol/L glutamate, 10 mmol/L hepes, 100 U/mL penicillin and 100 μg/mL streptomycin. After 3 to 4 h the rings stuck to the bottom of the 6-well dishes and were covered with medium. After approximately 10 to 14 days, when cells had grown out from the aortic rings, the rings were removed and cells were passaged (i.e. passage 1) into 75 cm^2 cell culture flasks (Nunc, Roskilde, Denmark) using 0.05% trypsin and 0.02% EDTA. After having reached confluency after 5−7 days, cells were passaged (i.e. passage 2) into 24-well dishes (Corning, NY) to perform radioligand binding experiments.

B.6. Radioligand Binding. K_{ATP}-channels were radiolabeled with [^{3}H]-P 1075 (N-cyano-N′-[1,1-dimethyl-[2,2,3,3-^{3}H] propyl)-N"-(3-pyridinyl) guanidine,[44,45] with a specific activity of 108 Ci/mmol. The binding observed in the presence of 1 μmol/L P 1075 was regarded as nonspecific.

Membranes were incubated in a buffer containing 100 mmol/L TRIS·HCl (pH 7.4), 5 mmol/L $MgCl_2$, 1 mmol/L EGTA, 6 mmol/L ATP in a total volume of 200 μL. The concentration of receptor membranes was adjusted to a protein content of 100 μg per tube.[46] Bound radioligand was separated from free radioligand by rapid vacuum filtration through Whatman GF/A glass fiber filters. The filters were rapidly washed 8 times with 2 mL ice-cold buffer (10 mmol/L Tris, 5 mmol/L $MgCl_2$, pH 8.0).

Aortic cells cultivated in 24 well-plates were incubated in HBSS (Hanks' balanced salt solution) containing (mmol/L) 137 NaCl, 5.4 KCl, 1.2 $MgSO_4$, 0.34 Na_2HPO_4, 4.2 $NaHCO_3$, 0.44 KH_2PO_4, 20 HEPES, 5.5 glucose, 1.3 $CaCl_2$. The reaction was started by addition of the radioligand and stopped by suction of the incubation medium followed by 5 successive washings with cold Krebs-solution. The cell-bound ligand is transferred to scintillation vials after incubation of the cell monolayers with 1 mol/L NaOH for 30 min at 60 °C. After addition of 3 mL scintillation fluid (Ultima Gold, Packard, USA) the vials were vigorously shaken for 1 h and counted in a scintillation-counter (Packard 1500) with 50% efficiency.

Competition binding experiments were performed in the presence of 1 nmol/L [^{3}H]-P 1075 ([L*]) and increasing concentrations of competing ligands [L]. Displacement curves were analyzed by nonlinear regression as reported[47,48] according to the following equation

$$B_s([L]) = B_o - B_o\frac{[L]}{[L] + K_L(1 + [L^*]/K_L^*)} \qquad (4)$$

where B_o and $B_s([L])$ represent the specific binding of L* to K_{ATP}-channels in the absence and presence of L, respectively, K_L* denotes the dissociation constant of the radioligand L*, and K_L is the equilibrium dissociation constant of the test compound L. Experimental data were analyzed after transformation of data to obtain homoscedasticity,[49] which resulted in reliable estimates of parameters (B_o, B_{ns}, and pK_D) and asymptotic standard deviations (ASD). Data were fitted to the hyperbola defined by eq 4 by nonlinear regression using the SAS software package STAT. Data points in the figures are means ± SEM.

B.7. Drugs and Materials. [^{3}H]-P 1075 (108 Ci/mmol = 4.00 TBq/mmol) was purchased from the Radiochemical Center, Amersham, U.K. Bimakalim, rilmakalim, and P 1075 were generous gifts from E. Merck (Darmstadt, FRG), Leo (Ballerup, Denmark), and Aventis AG (Frankfurt, FRG), respectively. Stock solutions of KCOs were dissolved in DMSO. DMSO attained a concentration in the organ bath not higher than 0.2% v/v and 1% in radioligand binding. Other chemicals were obtained from local commercial sources.

C. Chemical Descriptors. GRID independent descriptors (GRIND)[30] were used. GRIND start from molecular interaction fields (MIF) computed with the program GRID. The large body of information contained in these fields (on the order of some hundreds of thousands of grid points) is then encoded using the following method. The computation of GRIND involves a preliminary simplification of a few MIF to extract the main pharmacophoric regions, followed by a particular type of autocorrelation transform. The results are a small set of alignment-independent descriptors representing the internal geometrical relationship of such pharmacophoric regions. These can be used directly for the chemometric analysis and can be interpreted with the appropriate software,[30] using graphical representations of the pharmacophoric regions and their interactions, together with the molecular structures, in interactive 3D plots.

D. Statistical Approaches. PLS analysis[50] was performed with the GOLPE[51] software, version 3.1, on a Silicon Graphics workstation.

Acknowledgment. We are grateful to Prof. Dr. H. Hägele, Institute of Inorganic and Structural Chemistry, Heinrich-Heine-Universität Düsseldorf, for recording and discussing the ^{1}H NMR spectra. We thank Dagmar Grittner and Joachim Küper for performing the radioligand binding experiments.

Supporting Information Available: Table of crystal data and intensity collection and refinement details, tables of atomic coordinates, bond lengths and angles, anisotropic displacement parameters, hydrogen atom coordinates, torsion angles, and hydrogen bonds. This material is available free of charge via the Internet at http://pubs.acs.org.

References

(1) Isomoto, S.; Kondo, C.; Kurachi, Y. Inwardly rectifying potassium channels: Their molecular heterogeneity and function. *Jpn. J. Physiol.* **1997**, *47*, 11−39.
(2) Aguilar-Bryan, L.; Clement, J. P.; Gonzalez, G.; Kunjilwar, K.; Babenko, A.; Bryan, J. Toward understanding the assembly and structure of K_{ATP} channels. *Physiol. Rev.* **1998**, *78*, 227−245.
(3) Faivre, J. F.; Findlay, I. Action potential duration and activation of ATP-sensitive potassium current in isolated guinea-pig ventricular myocytes. *Biochim. Biophys. Acta* **1990**, *1029*, 167−172.
(4) Noma, A. ATP-regulated K^+-channels in cardiac muscle. *Nature* **1983**, *305*, 147−148.
(5) Dunne, W. J.; Petersen, O. H. Potassium selective ion channels in insulin secreting cells: physiology, pharmacology and their role in insulin secreting cell. *Biochim. Biophys. Acta* **1991**, *1071*, 67−82.
(6) Cook, D. L.; Hales, C. N. Intracellular ATP directly blocks K^+-channels in pancreatic β-cells. *Nature* **1984**, *311*, 271−273.
(7) Quayle, J. M.; Standen, N. B. K_{ATP}-chanels in vascular smooth muscle. *Cardiovasc. Res.* **1994**, *28*, 797−804.
(8) Standen, N. B.; Quayle, J. M.; Davies, N. W.; Brayden, J. E.; Huang, Y.; Nelson, M. T. Hyperpolarizing vasodilators activate ATP-sensitive K^+-channels in atrial smooth muscle. *Science* **1989**, *245*, 177−180.
(9) Amoroso, S.; Schmid-Antomarchi, H.; Fosset, M.; Lazdunski, M. Glucose, sulfonylureas and neurotransmitter release: Role of ATP-sensitive K^+-channels. *Science* **1990**, *247*, 852−854.
(10) Bernardi, H.; Fosset, M.; Lazdunski, M. Characterization, purification, and affinity labeling of the brain [^{3}H]glibenclamide-binding protein, a putative neuronal ATP-regulated K^+ channel. *Proc. Natl. Acad. Sci. U.S.A.* **1988**, *85*, 9816−9820.

(11) Atwal, K. S. Modulation of potassium channels by organic molecules. *Med. Res. Rev*. **1992**, *6*, 569−591.
(12) Inagaki, N.; Tsuura, Y.; Namba, N.; Masuda, K.; Gonoi, T.; Horie, M.; Seino, Y.; Mizuta, M.; Seino, S. Cloning and functional characterization of a novel ATP-sensitive potassium channel ubiquitously expressed in rat tissues, including pancreatic islets, pituitary, skeletal muscle and heart. *J. Biol. Chem*. **1995**, *270*, 5691−5694.
(13) Sakura, H.; Ämmälä, C.; Smith, P. A.; Gribble, F. M.; Ashcroft, F. M. Cloning and functional expression of the cDNA encoding a novel ATP-sensitive potassium channel subunit expressed in pancreatic β-cells, heart and skeletal muscle. *FEBS Lett*. **1995**, *377*, 338−344.
(14) Aguilar-Bryan, L.; Nichols, C. G.; Wechsler, S. W.; Clement, J. P.; Boyd, A.; E.; Gonzáles, G.; Herrera-Sosa, H.; Nguy, K.; Bryan, J.; Nelson, D. A. Cloning of the beta cell high-affinity sulfonylurea receptor: A regulator of insulin secretion. *Science* **1995**, *268*, 423−426.
(15) Inagaki, N.; Gonoi, T.; Clement, J. P., IV.; Nambe, N.; Inazawa, J.; Gonzalez, G.; Aguilar-Bryan, L.; Seino, S.; Bryan, J. A family of sulfonylurea receptors determines the pharmacological properties of ATP-sensitive K^+-channels. *Neuron* **1996**, *16*, 1011−1017.
(16) Isomoto, S.; Kondo, C.; Yamada, M.; Matsumoto, S.; Higashiguchi, O.; Horio, Y.; Matsuzawa, Y.; Kurachi, Y. A novel sulfonylurea receptor forms with BIR (Kir6.2) a smooth muscle type ATP-sensitive K^+-channel. *J. Biol. Chem*. **1996**, *271*, 24321−24324.
(17) Uhde, I.; Toman, A.; Gross, I.; Schwanstecher, C.; Schwanstecher, M. Identification of the Potassium Channel Opener Site on Sulfonylurea Receptors. *J. Biol. Chem*. **1999**, *274*, 28079−28082.
(18) Empfield, J. R.; Russell, K. Potassium channel openers. *Annu. Rep. Med. Chem*. **1995**, *30*, 81−89.
(19) Edwards, G.; Weston, A. H. Structure−activity relationships of K^+ channel openers. *Trends Pharmacol. Sci*. **1990**, *11*, 417−422.
(20) Bergmann R.; Gericke R. Synthesis and antihypertensive activity of 4-(1,2-Dihydro-2-oxo-1-pyridyl)-2*H*-1-benzopyrans and related compounds, new potassium channel activators. *J. Med. Chem*. **1990**, *33*, 492−504.
(21) Englert, H. C.; Wirth, K.; Gehring, D.; Furst, U.; Albus, U.; Scholz, W.; Rosenkranz, B.; Schoelkens, B. A. Airway pharmacology of the potassium channel opener, HOE 234, in guinea pigs: in vitro and in vivo studies. *Eur. J. Pharmacol*. **1992**, *210*, 69−75.
(22) Mannhold, R.; Cruciani, G.; Weber, H.; Lemoine, H.; Derix, A.; Weichel, C.; Clementi, M. 6-Substituted benzopyrans as potassium channel activators: synthesis, vasodilator properties and multivariate analysis. *J. Med. Chem*. **1999**, *42*, 981−991.
(23) Horino, H.; Mimura, T.; Kobayashi, S.; Ohta, M.; Kubo, H.; Ito, K.; Tsumura, M.; Kitagawa, M. Novel potassium channel opener prodrugs with a slow onset and prolonged duration of action. *Chem. Pharm. Bull*. **2000**, *48*, 490−495.
(24) Shindo, T.; Katayama, Y.; Horio, Y.; Kurachi, Y. MCC-134, a novel vascular relaxing agent, is an inverse agonist for the pancreatic-type ATP-sensitive K(+) channel. *J. Pharmacol. Exp. Ther*. **2000**, *292*, 131−135.
(25) Hambrock, A.; Löffler-Walz, C.; Kloor, D.; Delabar, U.; Horio, Y.; Kurachi, Y.; Quast, U. ATP-Sensitive K^+ channel modulator binding to sulfonylurea receptors SUR2A and SUR2B: opposite effects of MgADP. *Mol. Pharmacol*. **1999**, *55*, 832−840.
(26) Quast, U.; Bray, K. M.; Andres, H.; Manley, P. W.; Baumlin, Y.; Dosogne, J. Binding of the K^+ channel opener [^{3}H]P1075 in rat isolated aorta: relationship to functional effects of openers and blockers. *Mol. Pharmacol*. **1993**, *43*, 474−481.
(27) Mannhold, R.; Lemoine, H.; Jaspert, S. Comparison of binding and relaxant properties of potassium channel openers (KCO) in calf coronary arteries. *Naunyn-Schmiedeberg's Arch. Pharmacol*. **1996**, *353*, R54.
(28) Lemoine, H.; Teschemacher, A.; Mannhold, R.; Divanac'h, A. Binding studies with potassium channel openers in intact smooth muscle cells of calf trachea. *Naunyn-Schmiedeberg's Arch. Pharmacol*. **1997**, *355*, R267.
(29) Hambrock, A.; Löffler-Walz, C.; Russ, U.; Lange, U.; Quast, U. Characterization of a mutant sulfonylurea receptor SUR2B with high affinity for sulfonylureas and openers: differences in the coupling to Kir6.x subtypes. *Mol. Pharmacol*. **2001**, *60*, 190−199.
(30) Pastor, M.; Cruciani, G.; McLay, I.; Pickett, S.; Clementi, S. Grid Independent Descriptors (GRIND). A Novel Class of Alignment-Independent Three-Dimensional Descriptors. *J. Med. Chem*. **2000**, *43*, 3233−3243.
(31) Salamon, E.; Weber, H.; Mannhold, R.; Lemoine, H. 6-Sulfonyl substituted benzopyrans as potassium channel openers (KCO): synthesis and pharmacological properties in aortic rings, tracheal strips and cardiac cells of the rat. 2nd European Graduate Student Meeting, Frankfurt/Main, Germany, 2000.
(32) Frank, W.; Gelhausen, B.; Reiss, G. J.; Salzer, R. Untersuchungen an Systemen des Typs PCl3/MCl3/Aren (M = Al, Ga), I. Reaktionen mit Monohalogenbenzolen; Multikern-NMR-spektroskopische Charakterisierung von Aryldichlorhydrogenphosphoniumsalzen; Struktur des para-Fluorphenyldichlorphosphonium-tetrachloroaluminats. (Investigations on systems of the type PCl_3/MCl_3/arene (M = Al, Ga), I. Reactions with monohalobenzenes; multinuclear NMR-spectroscopic characterization of aryldichlorohydrogenphosphonium salts; crystal structure of *p*-fluorophenyldichlorophosphonium-tetrachloroaluminate). *Z. Naturforsch*. **1998**, *53b*, 1149−1168.
(33) Brandl, M.; Weiss, M. S.; Jabs, A.; Sühnel, J.; Hilgenfeld, R. C−H···π-Interactions in Proteins. *J. Mol. Biol*. **2001**, *307*, 357−377.
(34) McGaughey, G. B.; Gagné, M.; Rappé, A. K. π-Stacking Interactions. *J. Biol. Chem*. **1998**, *273*, 15458−15463.
(35) Davies, W.; Dick, J. H. Aromatic sulphonyl fluorides. A convenient method of preparation. *J. Chem. Soc*. **1931**, 2104−2109.
(36) Curtius, Th.; Rissom, J. Umsetzungen des Benzolsulfonazids. (Reactions of benzenesulfonylazide). *J. Prakt. Chem*. **1930**, *125*, 311−323.
(37) Petersen, S. Über neue Reaktionen von Sulfamiden (On new reactions of sulfonamides). *Ber. Dtsch. Chem. Ges*. **1950**, *83*, 551−558.
(38) Szeja, W. Synthesis of sulfonic esters under phase-transfer catalysed conditions. *Synthesis* **1979**, 822−823.
(39) Sheldrick, G. M. *SHELXS86. Program for the Solution of Crystal Structures*; Univerity of Göttingen: Göttingen, Germany, 1985.
(40) Sheldrick, G. M. *SHELXS97. Program for the Refinement of Crystal Structures*' Univerity of Göttingen: Göttingen, Germany, 1997.
(41) Blinks, J. Convenient apparatus for recording contractions of isolated muscle. *J. Appl. Physiol*. **1965**, *20*, 755−757.
(42) Lemoine, H.; Teng K. J.; Slee, S. J.; Kaumann, A. J. On minimum cyclic AMP formation rates associated with positive inotropic effect mediated through β_1-adrenoceptors in kitten myocardium. β_1-specific and non-adrenergic stimulant effects of denopamine. *Naunyn-Schmiedeberg's Arch. Pharmacol*. **1989**, *339*, 113−128.
(43) Ross, R. The smooth muscle cell. Growth of smooth muscle in culture and formation of elastic fibres. *J. Cell. Biol*. **1971**, *50*, 172−186.
(44) Manley, P. W.; Quast, U.; Andres, H.; Bray, K. Synthesis of and radioligand binding studies with a tritiated pinacidil analogue: receptor interactions of structurally different classes of potassium channel openers and blockers. *J. Med. Chem*. **1993**, *36*, 2004−2010.
(45) Quast, U.; Bray, K.; Andres, H.; Manley, P. W.; Baumlin, Y.; Dosogne, J. Binding of the K^+channel opener [^{3}H]-P1075 in rat isolated aorta: relationship to functional effects of openers and blockers. *Mol. Pharmacol*. **1993**, *43*, 474−481.
(46) Bradford, M. A rapid and sensitive method for the quantitation of microgram quantities of protein utilizing the principle of protein dye-binding. *Anal. Biochem*. **1976**, *72*, 248−254.
(47) Lemoine, H.; Ehle, B.; Kaumann, A. J. Direct labelling of β_2-adrenoceptors. Comparison of binding potency of ^{3}H-ICI 118,-551 and blocking potency of ICI 118,551. *Naunyn-Schmiedeberg's Arch. Pharmacol*. **1985**, *331*, 40−51.
(48) Lemoine, H. β-Adrenoceptor Ligands: Characterization and quantification of drug effects. *Quant. Struct.−Act. Relat*. **1992**, *11*, 211−218.
(49) Ehle, B.; Lemoine, H.; Kaumann, A. J. Improved evaluation of binding of ligands to membranes containing several receptor-subtypes. *Naunyn-Schmiedeberg's Arch. Pharmacol*. **1985**, *331*, 52−59.
(50) Wold, S.; Esbensen, K.; Geladi, P. Principal component analysis. *Chemom. Intell. Lab. Syst*. **1987**, *2*, 37−52.
(51) (a) Baroni, M.; Costantino, G.; Cruciani, G.; Riganelli, D.; Valigi, R.; Clementi, S. Generating Optimal Linear PLS Estimations (GOLPE): An Advanced Chemometric Tool for Handling 3D-QSAR Problems. *Quant. Struct.−Act. Relat*. **1993**, *12*, 9−20. (b) *GOLPE*, version 4.5; Multivariate Infometric Analysis Srl.: Viale dei Castagni 16, Perugia, Italy 1999.

JM010999G